ORIGINAL CONTRIBUTION

Effects of ionic strength on the size and compactness of chitosan nanoparticles

Helene Jonassen · Anna-Lena Kjøniksen · Marianne Hiorth

Abstract In this work, chitosan nanoparticles were prepared by ionotropic gelation of chitosan with tripolyphosphate (TPP). The effects of the ionic strength of the solvent employed in the particle preparation on the average size and compactness of the particles were investigated. In addition, the effects of the chitosan concentration and the crosslinker to polymer ratio on the particle characteristics were studied. The chitosan–TPP nanoparticles were characterized by dynamic light scattering, zeta potential, and turbidity measurements. The compactness of the nanoparticles was estimated with a method based on the size of the nanoparticles and the turbidity of the nanoparticle suspension. All the investigated preparation parameters, i.e., the ionic strength of the solvent, the chitosan concentration, and the TPP to chitosan ratio, affected the particle characteristics. For instance, smaller and more compact particles were formed in saline solvents, compared to particles formed in pure water. Further, the addition of monovalent salt rendered it possible to prepare particles in the nanometer size range at a higher polymer concentration. Solvent salinity is thus an important parameter to address in the preparation of chitosan nanoparticles crosslinked with TPP.

Keywords Nanoparticles · Chitosan · Tripolyphosphate · Ionic strength · Particle size · Particle compactness

Introduction

Chitosan refers to a series of semi-synthetic biopolymers obtained by deacetylation of the naturally occurring polysaccharide chitin. Chitosan is composed of β-1,4-linked glucosamine and N-acetyl-D-glucosamine units, and is mainly characterized by the amount of deacetylated units and by its molecular weight. The degree of deacetylation (DDA) usually ranges from 70 to 95%, while the molecular weight varies widely from 10 to 1000 kDa [1]. The amine groups on the polymer backbone can be protonated in an acidic environment, rendering the polymer positively charged and water soluble. The pK_a value of chitosan has been reported to be around 6.3–6.6 [2–4], and its solubility above this value is limited. The use of acidic solvents can be avoided by utilizing water soluble salt derivatives of chitosan, such as chitosan chloride.

Chitosan has been reported to be biocompatible and biodegradable, and has been applied in many different drug formulations ranging from gels to tablets, capsules and micro- and nanoparticles [5, 6]. In order to improve or modulate the characteristics of chitosan based drug formulations, chemical or physical crosslinking may be applied. Of these options, physical crosslinking is usually preferred, since less toxicity concerns arise when the chemical nature of the components remains unaltered, and because chemical crosslinking agents often are toxic in nature [5]. Furthermore, the often mild conditions under which physical crosslinking is performed [4, 5, 7], render this method more applicable to encapsulation of labile drugs.

Chitosan nanoparticles of different compositions (both chemically and physically crosslinked) have been studied for improving the treatment of a variety of diseases. For instance, glycol chitosan based nanoparticles have recently shown promising results for both diagnostic and therapeutic [8, 9] purposes in cancer treatment.

In cancer diagnosis and therapy, the biodistribution of the nanoparticles after intravenous injection is highly important - the goal is to achieve complete targeting to the tumor and to avoid deposition of the nanoparticles in normal tissue. Generally, particles in the size range 10 to 500 nm have longer

H. Jonassen (✉) · A.-L. Kjøniksen · M. Hiorth
Department of Pharmacy, School of Pharmacy, University of Oslo,
P.O. Box 1068 Blindern, 0316 Oslo, Norway
e-mail: helene.jonassen@farmasi.uio.no

circulation times and may deposit in tumor tissue by either active targeting or by the enhanced permeation and retention effect [10]. However, particles above approximately 200 nm must have some kind of deformability in order to avoid deposition in the spleen, were fenestrations typically are 200–500 nm in width [11]. These considerations, combined with the effects of the particle size and compactness on drug release rates [12–14], highlight the importance of estimating both the size and the compactness (or deformability) of nano-particulate drug delivery systems. However, in contrast to the particle size, the particle compactness is seldom reported. This might be due to experimental difficulties in determining the compactness of such small particles [15]. Recently, a method for the estimation of the local polymer concentration inside spherical nanoparticles (i.e. the compactness) based on the size of the nanoparticles and the turbidity of the nanoparticle suspension was published [15]. By applying this method, valuable information about the compactness of the nanopar-ticles is obtained, and a more complete physico-chemical characterization of the nanoparticles may be performed.

Chitosan can be physically crosslinked with both high molecular weight polyanions and low molecular weight mul-tivalent anions [1, 4, 5]. A commonly used example of the latter is tripolyphosphate (TPP), which has been recognized by the U.S. Food and Drug Administration as an acceptable food additive [16]. Depending on the pH, the TPP-anions can possess up to five negative charges [17] and may crosslink the protonated amine groups on the chitosan backbone by electrostatic forces – either between groups on the same poly-mer chain (intra-crosslinks) or on different polymer chains (inter-crosslinks). Depending on the preparation parameters, particles in the micro- or nanometer range can be made by such physical crosslinking of chitosan with TPP [18, 19]. In order to make nanoparticles, the ionic gelation should be performed in the dilute polymer concentration regime, so that a local gela-tion process within small polymer coils or polymer aggregates is insured. In contrast, performing the gelation process in the semi-dilute regime, where the polymer chains are overlapping, would lead to the formation of much larger particles or a macroscopic gel. Chitosan nanoparticles crosslinked with TPP (chitosan–TPP nanoparticles) have been employed in drug delivery of both small molecular drugs, like estradiol and venlafaxine, and macromolecules, such as insulin and DNA [4, 13, 17, 19–27], and is thus a promising nanoparticu-late drug delivery system. Several factors affecting the charac-teristics of chitosan–TPP nanoparticles have been studied, such as the ratio between crosslinker and polymer [17, 20–23, 28–30], the molecular weight of the chitosan [17, 20, 21, 24, 26–29], the chitosan concentration [22, 23, 26, 28, 31] and the pH [19, 22, 28, 29]. For instance, increasing the molecular weight and the concentration of the chitosan employed in the preparation of chitosan–TPP nanoparticles have resulted in the formation of larger particles [20–24, 26–29, 31]. While higher

TPP to chitosan ratios generally have resulted in smaller par-ticles [21–23, 28], with lower zeta potentials [21–23, 28, 29]. In addition, the adjustment of the pH of the chitosan solution used in the particle preparation from pH 4 to pH 5.5 has been shown to moderately reduce the size of the nanoparticles. Other attempts to tune the characteristics of chitosan–TPP nanoparticles have also been made, including varying the chitosan's DDA [29], changing the type of mechanical energy employed in the preparation [31], and by adjusting the solvent salinity [30]. Interestingly, for the latter case, the colloidal stability of the chitosan–TPP nanoparticles was shown to be enhanced by the presence of monovalent salt, resulting in narrower particle size distributions [30]. The study also im-plied that the addition of monovalent salt resulted in more compact particles. However, no attempts to estimate the parti-cle compactness were made.

The aim of this study was to further investigate the effects of ionic strength on the size and compactness of chitosan–TPP nanoparticles. Particles prepared in water were includ-ed as a reference. In addition, two other preparation param-eters that were considered likely to affect either the size or the compactness of the nanoparticles were included; the polymer concentration and the crosslinker to polymer ratio.

Experimental part

Materials

An ultrapure form of chitosan (chitosan chloride, PROTA-SAN™ UP CL 213) was chosen and purchased from Nova-matrix, FMC Biopolymer, Norway. The DDA of the chitosan was 83%. The weight average molecular weight (M_w) of the chitosan was $3.1*10^5$ Da and the polydispersity (M_w/M_n) 2.7, as determined by asymmetric flow field-flow fractionation (AFFFF; see below and Fig. 1). Tripolyphosphate (sodium triphosphate pentabasic, purum p.a. grade, $\geq 98.0\%$) was pur-chased from Sigma-Aldrich. Sodium chloride (for parenteral use) was supplied from Apotekproduksjon AS, Norway. The water used was purified with a Millipore Milli-Q system to insure minimal salt residues and total organic carbon (TOC).

Characterization of chitosan by AFFFF

The asymmetric flow field-flow fractionation (AFFFF) measurements were carried out on an AF2000 FOCUS system (Postnova Analytics, Landsberg, Germany) equipped with an RI detector (PN3140, Postnova) and a multiangle (seven detectors in the range 35–145°) light scattering detector (PN3070, $\lambda=635$ nm, Postnova). The sample (0.5 % w/w in 0.01 M NaCl) was measured using a 350 μm spacer, a regenerated cellulose membrane with a cutoff of 1000 (Z-MEM-AQU-425 N, Postnova), and an
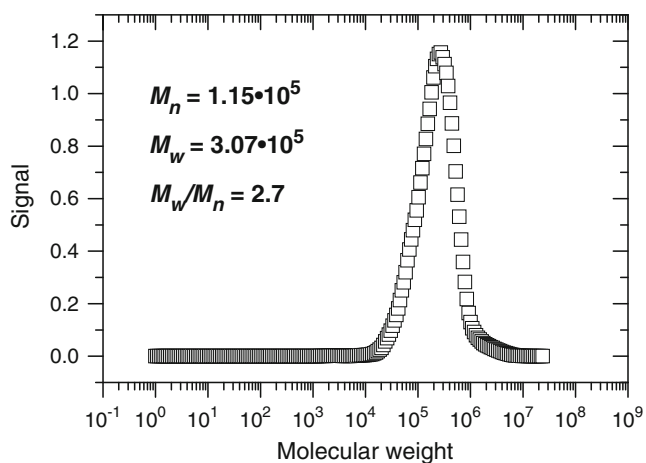
Fig. 1 The molecular weight distribution of chitosan determined by AFFFF. The calculated number average molecular weight (M_n) and the weight average molecular weight (M_w), along with the polydispersity index (M_w/M_n), are also given in the figure

injection volume of 20 μL. In the experiments, a constant detector flow rate of 5.0 mL/min, and a slot pump flow rate of 0.5 mL/min was used. The focusing time was 3 minutes at a cross-flow of 2 mL/min. The cross-flow was then reduced to zero during a period of time of 20 minutes. Processing of the measured data was achieved by the Postnova software (AF2000 Control, version 1.1.011). The molecular weight of the sample was determined using this software with a Zimm-type fit.

Experimental design

The experimental design applied in this study included three factors important for the nanoparticle characteristics; the chitosan concentration, the TPP:chitosan ratio and the ionic strength of the solvent (see Table 1). Different levels of the factors were used, resulting in a total of 30 different combinations. The combinations included chitosan samples without TPP present. The TPP:chitosan ratios were employed as weight:weight (w:w) ratios. The chitosan (chloride) concentrations given in table 1, 0.05 and 0.10% *w/w*, were the concentrations in the final solutions/suspensions. The solvents employed were water, 0.05 M NaCl and 0.15 M NaCl.

Table 1 The experimental design

Factor	Levels
Chitosan concentration (%, *w/w*)	0.05, 0.10
TPP:chitosan ratio (*w:w*)	0:100, 5:95, 10:90, 15:85, 20:80
Solvent	Water, 0.05 M NaCl, 0.15 M NaCl

Preparation of particles

Chitosan–TPP nanoparticles were produced by ionic gelation, based on the method previously reported by Ma et al. [19]. TPP and chitosan (chloride) were initially dissolved in the same solvent (either water, 0.05 M NaCl or 0.15 M NaCl), and by the means of a peristaltic pump, a defined amount of TPP solution was added dropwise to a defined amount of dilute chitosan solution under magnetic stirring at room temperature. The concentration of the TPP solution prior to mixing was varied in order to make particles at the chosen TPP:chitosan ratios given in Table 1. The speed of the peristaltic pump (25 rpm) and magnetic stirring (550 rpm) were held constant, along with the batch size and the size of the tubing, vials and magnets used in the preparation. In order to avoid dust, all solutions were filtered into pre-rinsed vials before mixing the polymer and crosslinker solutions. The chitosan solutions were filtered using 5 micrometers (Millipore) syringe filters, while all other solutions were filtered using 0.22 micrometer (Millipore) syringe filters. The prepared chitosan particles were characterized without any further purification or alteration, by dynamic light scattering (DLS), turbidity and zeta potential measurements one day after preparation, and by pH measurements two days after preparation.

Zeta potential measurements

The zeta potential measurements were conducted at 25 °C on a Malvern Zetasizer 3000HSA. The instrument determines the electrophoretic mobility of the sample by the means of Laser Doppler Velocimetry and calculates the zeta potential from such measurements on the basis of the Henry equation relating the zeta potential, ζ, to the electrophoretic mobility, U_E, as follows:

$$U_E = \frac{2\varepsilon\zeta}{3\eta}f(Ka) \tag{1}$$

where η and ε are the viscosity and the dielectric constant, respectively, of the solvent at the given temperature. The Smoluchowski approximation to Henry's function ($f(Ka) = 1.5$) was applied. The viscosity and dielectric constant of the solvent were set as for water. Measurements were performed at the least in duplicate, with 5 consecutive runs on each replicate to insure repeatable results. The measuring time was set to automatic and zero field correction was performed on all measurements. The zeta potential values are given as the averages calculated on the basis of repeatable runs. It was not possible to measure the zeta potential of pure chitosan in solution (combinations with crosslinker:polymer ratio 0:100)

due to low signals, irrespective of the polymer concentration and solvent employed.

pH measurements

The pH of the samples was measured at room temperature using a Mettler Toledo 220 pH Meter (calibrated with buffer pH 4 and pH 7).

Dynamic light scattering measurements

DLS measurements were performed with an ALV/CGS-8F Compact Goniometer System, with 8 fiber-optical detection units, from ALV-GmbH, Langen, Germany at 25 °C. A more detailed description of the instrumentation can be found elsewhere [32].

Particles scatter light according to their shape and size, and by the means of DLS measurements the particle size is derived on the basis of their Brownian motion. Assuming that the scattering of the incoming light exhibits Gaussian statistics, the experimentally measured homodyne intensity autocorrelation function $g^2(q,t)$ is directly linked to the theoretically amenable first-order electric field autocorrelation function $g^1(t)$ through the Siegert relationship [32–34]:

$$g^2(q,t) = 1 + B|g^1(t)|^2 \quad B \leq 1 \tag{2}$$

where B is an instrumental parameter, t is the time, and q is the wave vector defined as $q=4\pi n \sin(\theta/2)/\lambda_L$, where λ_L is the wavelength of the incident light in vacuum, θ is the scattering angle and n is the refractive index of the sample. In this work, n was measured with a PTR 46 refractometer from Index Instruments, UK.

In the analysis of the correlation functions, $g^1(t)$ was fitted to a stretched exponential function:

$$g^1(t) = \exp\left[-(t/\tau_{fe})^\beta\right] \quad 0 < \beta \leq 1 \tag{3}$$

where τ_{fe} is an effective relaxation time and β is a fitting parameter that gives an indication of the distribution width of the relaxation times (and thus the size distribution). High β values correspond to narrow size distributions. A fit was considered satisfactory with $r^2 > 0.997$.

The mean relaxation time is given by:

$$\tau_f = \frac{\tau_{fe}}{\beta} \Gamma \frac{1}{\beta} \tag{4}$$

where $\Gamma(1/\beta)$ is the gamma function. If the relaxation mode is diffusive, the mutual diffusion coefficient, D, is equal to $1/\tau_f q^2$, and the apparent hydrodynamic radius, R_h, can be calculated using the Stokes-Einstein relationship:

$$R_h = \frac{k_B T}{6\pi\eta D} \tag{5}$$

where k_B is the Boltzmann constant, T is the absolute temperature, and η is the viscosity of the solvent at the given temperature. The viscosity of water was applied irrespective of the solvent employed in the preparation of the particles.

The prepared chitosan–TPP nanoparticles were found to exhibit diffusive relaxation modes in almost all cases (R_h is independent of the scattering angle). But since small variations in the calculated values might occur depending on the angle, R_h was calculated at 90° for all samples in order to make a systematic comparison of the data. The sizes reported in this paper will be slightly overestimated, as soft particles have lower mutual diffusion coefficients than hard particles due to frictional reasons [35].

In order to evaluate the effect of the crosslinker amount on the apparent hydrodynamic radius of the particles prepared, normalized values of R_h at the different TPP:chitosan ratios were calculated by dividing the R_h at the given TPP:chitosan ratio by the R_h value at the ratio 5:95 (same chitosan concentration and solvent) as follows:

$$R_{h(normalized)} = \frac{R_{h(TPP:chitosan)}}{R_{h(5:95)}} \tag{6}$$

Turbidimetry

The transmittance of the prepared samples was measured at room temperature (ca. 25 °C) with a Helios Gamma (Thermo Spectronic, Cambridge, UK) spectrophotometer at a wavelength (λ_T) of 500 nm. The turbidity (τ) was calculated from the transmittance using Lambert-Beer's law:

$$\tau = -\frac{1}{L} \ln\left(\frac{I_t}{I_0}\right) \tag{7}$$

where L is the light path length in the sample cell (1 cm), I_t is the intensity of the light transmitted through the sample, and I_0 is the intensity of the light transmitted through the solvent (water). Measurements were performed at least in duplicate, and the reported values are the averages.

Determination of the particle compactness

A recently reported method was applied to calculate the particle compactness [15]. The method can be used to estimate the local polymer concentration inside nanoparticles (i.e. the particle compactness), along with the number density of particles in suspension, the molecular weight of the particles and the aggregation number of polymer chains in the nanoparticles, from the size of the nanoparticles and the turbidity of the nanoparticle suspension. The following equation was applied to

calculate the local polymer concentration, c_{NP}, inside the nanoparticles:

$$\tau = \frac{3c_t}{2c_{NP}R_h}\left[1 - \frac{2}{wc_{NP}}\left(\sin(wc_{NP}) - \frac{1}{wc_{NP}}(1 - \cos(wc_{NP}))\right)\right] \quad (8)$$

where τ is the turbidity of the nanoparticle suspension, R_h is the apparent hydrodynamic radius of the particles, c_t is the total polymer concentration in suspension, and w is $w = \frac{4\pi R_h(dn/dc)}{\lambda_T n_0}$. λ_T is the wavelength at which the turbidity measurements were performed, n_0 is the refractive index of the solvent, and dn/dc is the refractive index increment of the polymer. The dn/dc has previously been determined to be 0.157 g/mL for this type of chitosan using the AFFFF instrumentation described above [15]. In order to apply this method, the total polymer concentration that is in the form of nanoparticles must be known. It was therefore assumed in this study that practically all chitosan was in the form of nanoparticles. The method is developed for monodisperse particles, and if applied on particles exhibiting broader size distributions, larger deviations in the data will naturally occur.

Determination of the aggregation number of polymer chains in the nanoparticles

The aggregation number of polymer chains in the nanoparticles, N_{agg}, was determined from the following equation [15]:

$$N_{agg} = \frac{M_{NP}}{M_n} \quad (9)$$

where M_n is the number average molecular weight of the polymer. M_{NP} is the molecular weight of the particles and is expressed as:

$$M_{NP} = \frac{4}{3}\pi R_h^3 c_{NP} N_A \quad (10)$$

where R_h is the apparent hydrodynamic radius of the particles, c_{NP} is the local polymer concentration inside the particles and N_A is Avogadro's number.

In order to evaluate the effect of the crosslinker amount on the aggregation number of polymer chains in the particles, normalized values of N_{agg} at the different TPP:chitosan ratios were calculated by dividing the N_{agg} at the given TPP:chitosan ratio by the N_{agg} value at the ratio 5:95 (same chitosan concentration and solvent) as follows:

$$N_{agg(normalized)} = \frac{N_{agg(TPP:chitosan)}}{N_{agg(5:95)}} \quad (11)$$

Results

Characterization of chitosan

The results from the AFFFF experiments showed that the chitosan investigated in this work exhibited a medium molecular weight and a quite high polydispersity index (see Fig. 1). The weight average molecular weight (M_w) and number average molecular weight (M_n) were estimated to be $3.07*10^5$ and $1.15*10^5$, respectively. The polydispersity index (M_w/M_n) was calculated to be 2.7. The molecular weight estimated was in accordance with the supplier's information (M_w between 100–400 kDa), and the polydispersity was as expected for a semi-synthetic polymer of natural origin.

DLS experiments were conducted to investigate the effect of salt on the average hydrodynamic radius of pure chitosan in aqueous solution (in the absence of the TPP crosslinker). It was, however, difficult to obtain reproducible correlation functions since the polymer solutions scattered little light as a result of the low concentrations used. The hydrodynamic radius of pure chitosan in solvents of different ionic strength (water, 0.05 M NaCl and 0.15 M NaCl) was for that reason not calculated. Some large differences between the investigated samples could, however, be found on the basis of the obtained correlation functions (see Fig. 2 for the samples with the highest chitosan concentration). For instance, the relaxation times were highly affected by the salinity of the solvent; longer relaxation times were found when chitosan (chloride) was dissolved in pure water, compared to saline solvents. However, there was no pronounced difference in relaxation times between chitosan (chloride) dissolved in 0.05 M and 0.15 M NaCl, irrespective of the polymer concentration used. The intensity of the scattered light was higher when the ionic strength of the solvent was increased from 0 to 0.05 M NaCl and again to 0.15 M NaCl. This may be explained by the presence of more compact polymer entities in the solution. In water, the relaxation times observed for 0.10% chitosan solutions were longer than for 0.05% solutions (data not shown). This indicates that the aggregation of chitosan chains was more pronounced at the higher chitosan concentration.

Particle preparation and characterization

Table 1 gives an overview of the experimental design and the different combinations prepared. Nanoparticles were successfully formed for all combinations prepared under saline conditions, and the average hydrodynamic radius of the particles ranged from approximately 70 to 220 nm (see Fig. 3b for R_h). For the combinations prepared in water, either quite large particles were formed, with R_h values ranging from 470 to 1700 nm, or phase separation occurred
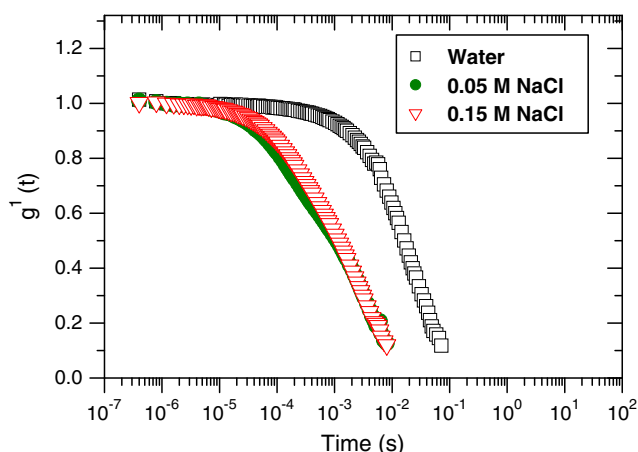
Fig. 2 The first-order electric-field autocorrelation functions, $g^I(t)$, for 0.10% chitosan dissolved in water, 0.05 M NaCl, and 0.15 M NaCl (without crosslinker present; TPP:chitosan ratio 0:100)

(see Fig. 3a). Phase separation was observed immediately/ one day after preparation for combinations prepared in water with high polymer concentration and the two highest cross-linker concentrations (TPP:chitosan ratios of 15:85 and 20:80). These combinations are therefore omitted from all figures. The ionic strength of the solvent clearly affected the average R_h of the particles prepared. Increasing the ionic strength of the solvent to a medium level of 0.05 M NaCl resulted in much smaller particles at both polymer concentrations and all TPP:chitosan ratios employed. A further increase in the ionic strength of the solvent to 0.15 M NaCl resulted in larger particles with respect to the ones formed at a medium ionic strength, but much smaller than the ones formed in water. For all solvents and crosslinker concentrations, a pronounced rise in the average hydrodynamic radius of the particles was observed when the polymer concentration was increased (see Fig. 3a, b). The smallest particles were formed when low polymer concentration was combined with medium ionic strength solvent.

The effect of the crosslinker to polymer ratio on the average R_h of the particles prepared in saline solvents is illustrated in Fig. 3c with normalized R_h values. No significant changes in R_h at the lower crosslinker concentrations were observed for combinations with low polymer concentration irrespective of the solvent employed (0.05 or 0.15 M NaCl), but a marked decrease in R_h was observed when the TPP:chitosan ratio was increased to 20:80. For the particles prepared with high polymer concentration in saline solvents, an increase in R_h with increasing TPP:chitosan ratios up to 15:85 was found, followed by a decrease in R_h with further addition of TPP up to the ratio 20:80.

Using the two-tailed Student's t-test, it was found that particles prepared under saline conditions had significantly ($p<0.05$) narrower particle size distributions (β values 0.85–0.97) than particles prepared in pure water (β values
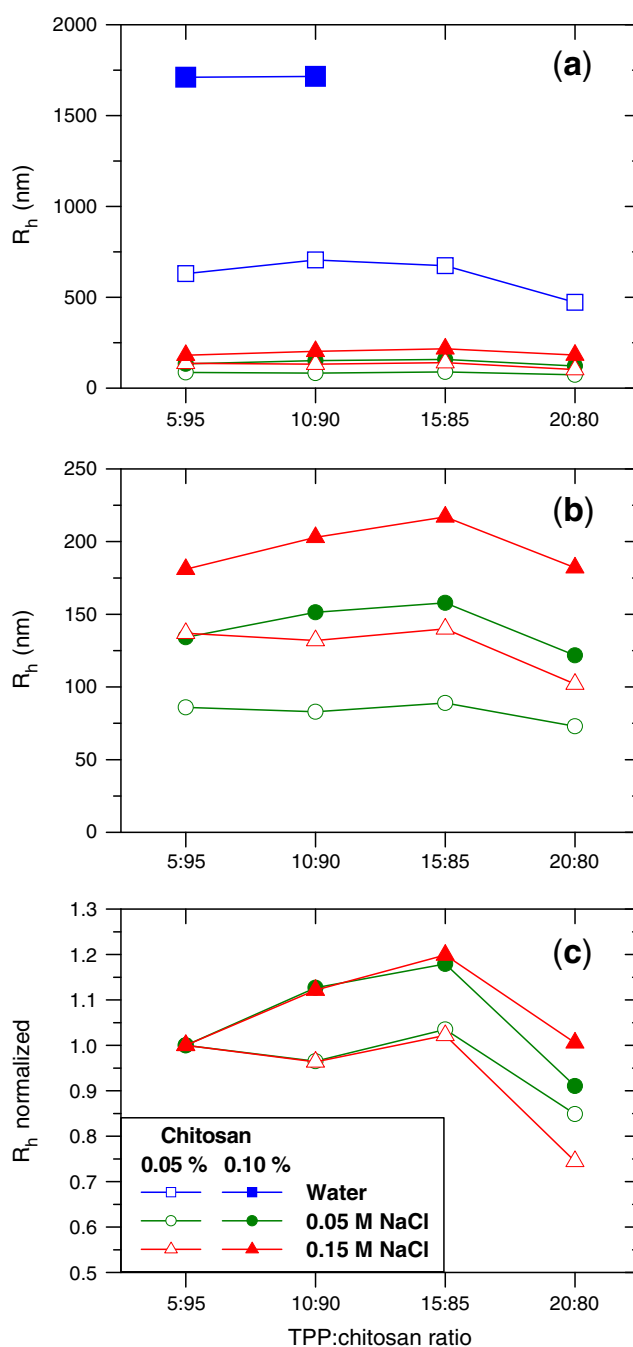

Fig. 3 The apparent hydrodynamic radius, R_h, as a function of TPP: chitosan ratio for **a** all particles prepared, **b** particles prepared under saline conditions, and **c** particles prepared under saline conditions normalized against the R_h value at the TPP:chitosan ratio 5:95. The combinations with 0.10% chitosan in water at the highest crosslinker concentrations had phase-separated after 1 day and are therefore omitted from **a**. Connection *lines* between the symbols are added in order to guide the eyes. The standard deviations of R_h are equal to or smaller than the size of the symbols

0.76–0.84). Applying the same two-tailed t-test also revealed that nanoparticles prepared in 0.15 M NaCl exhibited significantly ($p<0.05$) narrower particle size distributions than nanoparticles prepared in 0.05 M NaCl.

There was also a tendency towards narrower particle size distributions (higher β values) with increasing TPP:chitosan ratios for particles prepared in saline solvents. For particles prepared in water, the trend was reversed as a tendency towards broader particle size distributions were found with increasing TPP:chitosan ratios.

As can be seen in Fig. 4a, all the particles prepared in this study exhibited positive zeta potentials. The particles prepared in water had significantly higher average zeta potentials than the particles prepared in saline solvents. For the particles prepared in water, a marked decrease in the zeta potential values with increasing crosslinker concentrations was found. A similar but less pronounced trend could be observed for particles made under moderate amounts of salt (0.05 M NaCl), but as the ionic strength of the solvent was further increased (to 0.15 M NaCl), the trend faded off.

For the nanoparticles prepared in saline solvents, the pH values of the final suspensions varied within approximately one pH unit, from 5.3 to 6.5. Generally, a slight increase in pH was observed with increasing TPP:chitosan ratios and by adjusting the solvent salinity from 0.05 to 0.15 M NaCl. The chitosan concentration did not have much influence on the pH values of the nanoparticle suspensions in saline solvents. For the combinations prepared in water, the pH values ranged from approximately 4.3 to 6.8, and a more pronounced increase in pH was observed with increasing TPP:chitosan ratios. At high TPP:chitosan ratios, an increase in the chitosan concentration resulted in slightly higher (ca. 0.5 units) pH values in the final suspensions.

The calculated turbidity values of the prepared nanoparticle suspensions can be found in Fig. 4b. As expected, higher turbidity values were found for nanoparticles prepared with high polymer concentration, compared to particles prepared with low polymer concentration. Generally, increasing crosslinker concentrations resulted in higher turbidity values, especially for particles prepared under saline conditions and high polymer concentration.

The estimated local polymer concentrations inside the particles, c_{NP}, are given in Fig. 5a. It was found that an increase in the TPP:chitosan ratio resulted in a higher local polymer concentration inside the particles, irrespective of the solvent employed. It was further observed that an increase in the ionic strength of the solvent also resulted in a higher local polymer concentration. The chitosan concentration used, 0.05 or 0.10%, had no pronounced effects on the local polymer concentration inside the particles in saline solvents at low to moderate TPP:chitosan ratios (5:95, 10:90 and 85:15). But at the highest TPP:chitosan ratio employed, increasing the chitosan concentration from 0.05% to 0.10% resulted in higher local polymer concentrations inside the nanoparticles.

In Fig. 5b, the calculated aggregation numbers of polymer chains in the particles, N_{agg}, are given. The N_{agg} was increased when the chitosan concentration was raised from 0.05 to 0.10%, irrespective of the solvent and TPP:chitosan ratio employed. Furthermore, increasing TPP:chitosan ratios generally resulted in a rise in the N_{agg} before flattening out at the highest TPP:chitosan ratio (20:80). For both chitosan concentrations, increasing the ionic strength of the solvent to 0.05 M NaCl resulted in a dramatic decrease in the aggregation numbers. However, a further increase of the solvent's ionic strength to 0.15 M NaCl resulted in medium values of aggregation numbers. As can be seen in Fig. 5c for the particles prepared in saline solvents, the increase in normalized N_{agg} values was more pronounced at high polymer concentration than at low polymer concentration.
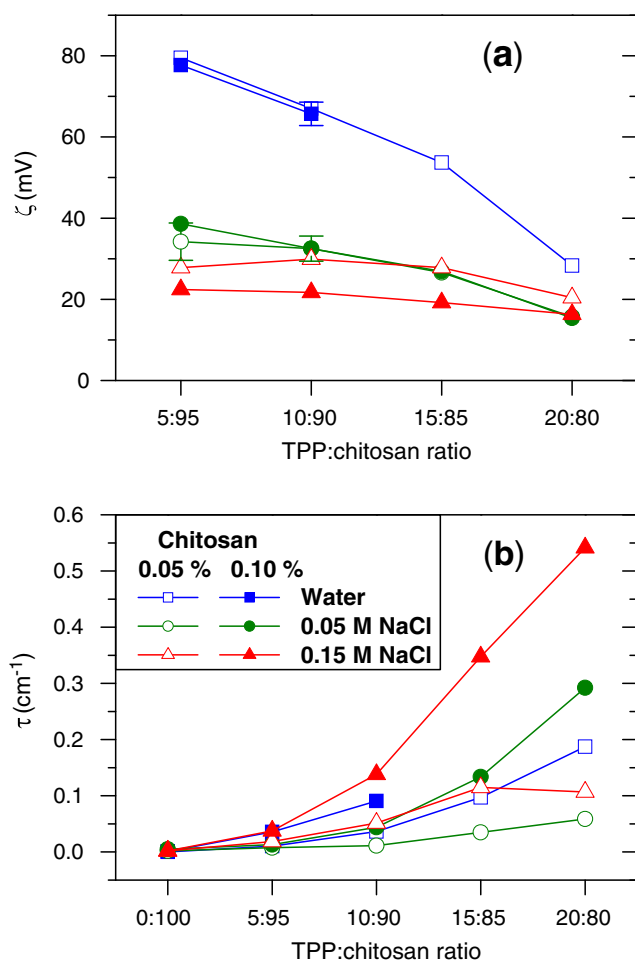

Fig. 4 The average values of **a** the zeta potential of the particles and **b** the turbidity of the solutions/suspensions as a function of TPP:chitosan ratio. Connection *lines* between the symbols are added in order to guide the eyes. Samples in which phase separation was observed are omitted from the plots. The *points* without error bars have standard deviations equal to or smaller than the size of the symbols
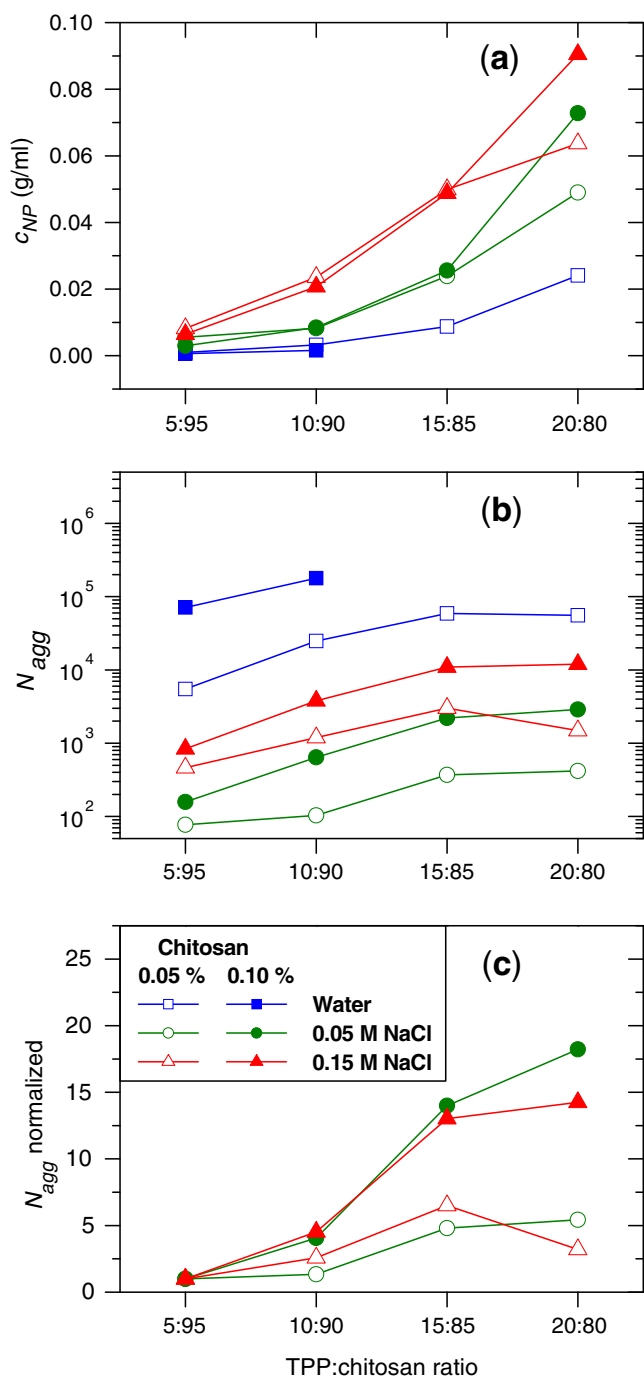
Fig. 5 **a** The estimated local polymer concentration inside the particles, c_{NP}, **b** the calculated aggregation number of polymer chains in the particles, N_{agg}, and **c** the normalized aggregation number of polymer chains in the particles prepared in saline solvents as a function of TPP:chitosan ratio. Connection *lines* between the symbols are added in order to guide the eyes. Samples in which phase separation was observed are omitted from the figure

Discussion

In aqueous solution, the highly protonated chitosan has been reported to have a rather stiff and extended conformation [6,

25] due to the electrostatic repulsion between the positively charged amine groups on the chitosan backbone. These charges may be screened out when a monovalent salt like sodium chloride is added to the solvent. This salt-induced screening effect will lead to reduced electrostatic repulsion between the charged groups on the polymer backbone and hence increased flexibility of the polymer chains in solution. The formation of smaller, more compact and coil-like polymer entities will thus be encouraged in saline solvents, as opposed to deionized water. The observation of larger polymer entities made for chitosan samples prepared in water, compared to saline solvents (Fig. 2), supports this hypothesis. This is also in accordance with a previous report on the effect of ionic strength on the conformation of chitosan in solution [36], where it was found that the intrinsic viscosity of chitosan decreased with increasing ionic strength of the solution. The authors explained this by the contraction of the chitosan molecules due to increased charge screening in high ionic strength solutions. As already mentioned in the results section, the intensity of the scattered light from the chitosan solutions was higher with increasing ionic strength of the solvent. This supports the presence of more compact polymer entities in solution in saline solvents with respect to pure water.

In this work, chitosan nanoparticles were prepared using a well-known preparation method in which the positively charged chitosan is ionically crosslinked with negatively charged TPP-anions. Such chitosan nanoparticles have previously been reported to possess positive zeta potentials [13, 20–30, 37], which is in accordance with the results found in this study. But as can be seen in Fig. 4a, much lower zeta potentials were observed for particles prepared in saline solvents, compared to particles prepared in water. This can be explained by the salt-induced screening of charges when NaCl is present. The TPP-anions will, as a result of the crosslinker reaction, occupy some of the chitosan's positive charges. Therefore, a reduction in the average zeta potential of the particles was found with increasing TPP:chitosan ratios in water. However, in saline solvents, this trend was much less pronounced or not apparent, probably due to the salt-induced screening of the charges. These results are in agreement with the findings of Huang and Lapitsky [30]. Interestingly, Huang and Lapitsky argued that in spite of the lower zeta potentials, the surface charge density of the particles may be higher in the presence of 0.15 M NaCl than in pure water.

In the absence of NaCl and TPP, the chitosan entities in solution attained a swollen and extended conformation due to the electrostatic repulsion between the protonated amine groups. It has previously been reported that the binding of TPP with chitosan is stronger, and that it occurs at a faster rate, in the absence of monovalent salt [30]. In pure water, a fast and strong binding of TPP with extended chitosan

chains/entities in solution may therefore promote inter-chain crosslinking. This may explain the presence of large (Fig. 3a) particles with high aggregation numbers (Fig. 5b) observed for combinations prepared in water. Relatively low c_{NP} values were also found for these particles. This indicates that the swollen nature of the chitosan in solution, prior to the addition of TPP, is somewhat preserved during the crosslinking process.

The addition of a moderate amount of NaCl (0.05 M) screened out some of the repulsive electrostatic forces and induced contraction of the chitosan chains/entities in solution. As can be seen in Fig. 5a, this resulted in higher values of c_{NP} for particles prepared in 0.05 M NaCl with respect to particles prepared in water. In the presence of monovalent salt, the slow binding of TPP [30] with small and compact chitosan chains/entities in solution may reduce the tendency of inter-chain crosslinking. Accordingly, the aggregation numbers were lower for particles prepared in 0.05 M NaCl, than for the ones made in pure water (see Fig. 5b). Since the particles formed in 0.05 M NaCl had both lower values of N_{agg} and were more compact, the average particle size was also much smaller than for the particles made in pure water (see Fig. 3a, b).

Increasing the ionic strength of the solvent further, to 0.15 M NaCl, caused more efficient charge screening and contraction of the chitosan chains/entities in solution, and hence higher values of c_{NP} (Fig. 5a) were found for particles prepared under these conditions. It has previously been reported that an increase in the ionic strength of the media favors inter-chain association of chitosan molecules [38]. An increase in the ionic strength of the solvent may therefore promote aggregation. The increased N_{agg} values found for particles prepared at 0.15 M NaCl with respect to 0.05 M NaCl can therefore be explained by such salt-induced aggregation of the chitosan chains. As can be seen in Fig. 3b, the R_h was higher for particles prepared at 0.15 M NaCl than for particles prepared at 0.05 M NaCl. This illustrates that the aggregation-induced size increase was more dominating than the contraction-induced size decrease.

An increase in both R_h and N_{agg} was found when the chitosan concentration was increased. Such concentration-induced particle size increase has been found in several previous studies on chitosan–TPP nanoparticles [22, 23, 28, 31]. This is also in agreement with the DLS measurements of pure chitosan in water, where a significant increase in the relaxation time was observed when the polymer concentration was increased (data not shown), indicating the presence of larger polymer entities at higher chitosan concentration. However, as can be seen from Fig. 5a, increasing the polymer concentration did not affect the compactness of the particles at moderate TPP:chitosan ratios. This can be explained by the presence of the same amount of NaCl to screen the charges, and that the amount of

crosslinker with respect to the polymer is held constant. Assumingly, the contraction of the polymer will therefore be the same at both polymer concentrations. Interestingly, a deviation from this behavior was found at the highest TPP:chitosan ratio, where increasing the polymer concentration resulted in higher c_{NP}. In order to keep the TPP:chitosan ratio constant, the TPP concentration in the system is higher when the chitosan concentration is raised. This causes an increase in ionic strength which, at some point, might contribute significantly to the thermodynamic conditions of the polymer and in this way lead to higher contraction of the particles.

Shah and coworkers [23], along with Liu and Gao [22] observed in their studies on chitosan–TPP nanoparticles a decrease in particle size with increasing TPP:chitosan ratios. Interestingly, in our study increasing crosslinker concentrations affected the particle size in different manners, depending on the parameters chosen in the particle preparation (see Fig. 3a–c). The TPP-independent particle sizes observed at low polymer concentration and moderate crosslinker concentrations, may be a result of a combination of both enhanced aggregation (see Fig. 5b) and stronger contraction (see Fig. 5a) of the particles when the crosslinker concentration is raised. At the highest TPP:chitosan ratio, a decrease in R_h was found for both low and high chitosan concentration. At this stage, the particles continue to contract (see Fig. 5a), while the aggregation number is leveling out (see Fig. 5b). The overall result is therefore a reduction of the R_h. Further aggregation of the particles is probably suppressed at the highest crosslinker concentration, since the compactness of the particles and the already very high aggregation number will increase the time the particles need to be in contact with each other before they stick together [39-41]. At high polymer concentrations, the R_h increased with TPP:chitosan ratios up to 15:85, but the compactness was the same as for low polymer concentrations (Fig. 5a). As can be seen in Fig. 5c, the aggregation number increased faster when more crosslinker was added to the samples with high chitosan concentration, with respect to low chitosan concentration. The overall effect was therefore a size increase when more crosslinker was added.

Narrower particle size distributions (higher β values) were found with increasing ionic strengths. Huang and Lapitsky argued in their study that the narrower particle size distributions observed in the presence of NaCl was due to enhanced colloidal stability during nanoparticle formation [30]. They suggested that salt-mediated inhibition of bridging flocculation was the more likely cause of the anomalous salt effects on the colloidal stability of the chitosan–TPP nanoparticles. This was supported by the insensitivity of the zeta potential to TPP in the presence of 0.15 M NaCl, suggesting that few TPP-ions were binding to the nanoparticle surface. The aggregation of polymer nanoparticles

into larger aggregates has also been shown to be governed by the local polymer concentration inside the nanoparticles [39–42]. Previously, it has been argued that the formation of aggregates is dependent on the contact time between the particles when they collide (τ_c) and the time needed to obtain a permanent chain entanglement between the particles (τ_e) [42]. Consequently, the aggregate formation is suppressed when $\tau_c << \tau_e$. Tanaka [39, 40] has shown that the τ_e can be estimated, and that τ_e increases with the aggregation number of polymer chains in the particles and the volume fraction of polymer inside the particles (i.e. c_{NP}). Accordingly, aggregation is suppressed when the local polymer concentration inside the nanoparticles is sufficiently high. This reduced tendency towards aggregation induced by increasing c_{NP}, can also explain the reduction in particle size distribution observed with increasing solvent salinity.

The turbidity values are affected by the polymer concentration, the size of the particles and the compactness of the particles present (see Eq. 8). The aggregation of polymer chains or particles will lead to larger particles and hence higher turbidity values, in addition contraction will lead to more compact particles which also results in higher turbidity values. Particles that are both aggregating and contracting would accordingly cause the sample to become more turbid. However, the combined effect of the two processes can give rise to quite intricate effects on the turbidity values, as reflected in Fig. 4b. As expected, an increase in the polymer concentration leads to higher turbidity values (see Fig. 4b) due to higher aggregation (see Fig. 5b). In comparison, the effect of solvent salinity on the turbidity values was more intricate (see Fig. 4b), since the addition of NaCl can induce both aggregation and contraction. Increasing TPP:chitosan ratios could also have a rather intricate effect on the turbidity, however, increasing ratios generally lead to higher turbidity values. This can be explained by the rise in the compactness of the particles (see Fig. 5a) observed with increasing TPP:chitosan ratios, along with the almost TPP-independent R_h values found with increasing ratios.

Conclusions

This work has demonstrated that the ionic strength of the solvent used in the preparation of chitosan–TPP nanoparticles affects important particle characteristics. Large particles were formed when water was used as a solvent, while smaller particles were formed in 0.05 and 0.15 M NaCl. The smallest particles were formed in the medium ionic strength solvent, indicating that there is a non-linear relationship between the ionic strength of the solvent and the average size of the particles formed.

The study revealed that the average particle size of chitosan–TPP nanoparticles increased at high chitosan concentration,

and that increasing TPP:chitosan ratios resulted in only moderate changes in the average particle size in saline solvents. It was also found that the compactness of chitosan–TPP nanoparticles increased with higher solvent salinity, and with increasing TPP:chitosan ratios. However, no difference in the compactness of the particles prepared at high and low polymer concentration was observed when a moderate amount of cross-linker was employed. This indicates that the particle size can be adjusted to a preferred value by changing the polymer concentration, without affecting the compactness of the particles.

References

1. Hamman JH (2010) Chitosan based polyelectrolyte complexes as potential carrier materials in drug delivery systems. Mar Drugs 8 (4):1305–1322
2. Ravi Kumar MNV, Muzzarelli RAA, Muzzarelli C, Sashiwa H, Domb AJ (2004) Chitosan chemistry and pharmaceutical perspectives. Chem Rev 104(12):6017–6084
3. Anthonsen MW, Smidsrød O (1995) Hydrogen ion titration of chitosans with varying degrees of N-acetylation by monitoring induced 1H-NMR chemical shifts. Carbohyd Polym 26(4):303–305. doi:10.1016/0144-8617(95)00010-5
4. Park JH, Saravanakumar G, Kim K, Kwon IC (2010) Targeted delivery of low molecular drugs using chitosan and its derivatives. Adv Drug Del Rev 62(1):28–41. doi:10.1016/j.addr.2009.10.003
5. Dash M, Chiellini F, Ottenbrite RM, Chiellini E (2011) Chitosan—a versatile semi-synthetic polymer in biomedical applications. Prog Polym Sci 36(8):981–1014. doi:10.1016/j.progpolymsci.2011.02.001
6. Illum L (1998) Chitosan and its use as a pharmaceutical excipient. Pharm Res 15(9):1326–1331
7. Plapied L, Duhem N, des Rieux A, Préat V (2011) Fate of polymeric nanocarriers for oral drug delivery. Curr Opin Colloid Interface Sci 16(3):228–237. doi:10.1016/j.cocis.2010.12.005
8. Lee SJ, Koo H, Jeong H, Huh MS, Choi Y, Jeong SY, Byun Y, Choi K, Kim K, Kwon IC (2011) Comparative study of photosensitizer loaded and conjugated glycol chitosan nanoparticles for cancer therapy. J Contr Release 152(1):21–29. doi:10.1016/j.jconrel.2011.03.027
9. Na JH, Koo H, Lee S, Min KH, Park K, Yoo H, Lee SH, Park JH, Kwon IC, Jeong SY, Kim K (2011) Real-time and non-invasive optical imaging of tumor-targeting glycol chitosan nanoparticles in various tumor models. Biomaterials 32(22):5252–5261. doi:10.1016/j.biomaterials.2011.03.076
10. Koo H, Huh MS, Sun I-C, Yuk SH, Choi K, Kim K, Kwon IC (2011) In vivo targeted delivery of nanoparticles for theranosis. Acc Chem Res 44(10):1018–1028. doi:10.1021/ar2000138
11. Petros RA, DeSimone JM (2010) Strategies in the design of nanoparticles for therapeutic applications. Nat Rev Drug Discov 9 (8):615–627
12. Chouhan R, Bajpai AK (2010) Release dynamics of ciprofloxacin from swellable nanocarriers of poly(2-hydroxyethyl methacrylate): an in vitro study. Nanomedicine 6:453–462. doi:10.1016/j.nano.2009.11.006
13. Keawchaoon L, Yoksan R (2011) Preparation, characterization and in vitro release study of carvacrol-loaded chitosan nanoparticles. Colloids Surf B 84:163–171. doi:10.1016/j.colsurfb.2010.12.031
14. Kim S, Kim J-H, Kim D (2011) pH sensitive swelling and releasing behavior of nano-gels based on polyaspartamide graft copolymers. J Colloid Interface Sci 356:100–106. doi:10.1016/j.jcis.2011.01.003

15. Jonassen H, Kjøniksen A-L (2011) Optical-scattering method for the determination of the local polymer concentration inside nanoparticles. Phys Rev E 84(2):022401

16. Lin Y-H, Sonaje K, Lin KM, Juang J-H, Mi F-L, Yang H-W, Sung H-W (2008) Multi-ion-crosslinked nanoparticles with pH-responsive characteristics for oral delivery of protein drugs. J Contr Release 132(2):141–149

17. Ajun W, Yan S, Li G, Huili L (2009) Preparation of aspirin and probucol in combination loaded chitosan nanoparticles and in vitro release study. Carbohyd Polym 75(4):566–574

18. Mi F-L, Shyu S-S, Lee S-T, Wong T-B (1999) Kinetic study of chitosan–tripolyphosphate complex reaction and acid-resistive properties of the chitosan–tripolyphosphate gel beads prepared by in-liquid curing method. J Polym Sci Part B: Polym Phys 37 (14):1551–1564

19. Ma Z, Yeoh HH, Lim L-Y (2002) Formulation pH modulates the interaction of insulin with chitosan nanoparticles. J Pharm Sci 91:1396–1404. doi:10.1002/jps.10149

20. Csaba N, Koping-Hoggard M, Fernandez-Megia E, Novoa-Carballal R, Riguera R, Alonso MJ (2009) Ionically crosslinked chitosan nanoparticles as gene delivery systems: effect of PEGylation degree on in vitro and in vivo gene transfer. J Biomed Nanotechnol 5(2):162–171

21. Janes KA, Alonso MJ (2003) Depolymerized chitosan nanoparticles for protein delivery: preparation and characterization. J Appl Polym Sci 88(12):2769–2776. doi:10.1002/app.12016

22. Liu H, Gao C (2009) Preparation and properties of ionically cross-linked chitosan nanoparticles. Polym Adv Technol 20(7):613–619

23. Shah S, Pal A, Kaushik VK, Devi S (2009) Preparation and characterization of venlafaxine hydrochloride-loaded chitosan nanoparticles and in vitro release of drug. J Appl Polym Sci 112(5):2876–2887

24. Wang X, Chi N, Tang X (2008) Preparation of estradiol chitosan nanoparticles for improving nasal absorption and brain targeting. Eur J Pharm Biopharm 70(3):735–740

25. Wang X, Zheng C, Wu Z, Teng D, Zhang X, Wang Z, Li C (2009) Chitosan–NAC nanoparticles as a vehicle for nasal absorption enhancement of insulin. J Biomed Mater Res, Part B 88B(1):150–161

26. Wu Y, Yang W, Wang C, Hu J, Fu S (2005) Chitosan nanoparticles as a novel delivery system for ammonium glycyrrhizinate. Int J Pharm 295(1–2):235–245

27. Yang H-C, Hon M-H (2009) The effect of the molecular weight of chitosan nanoparticles and its application on drug delivery. Microchem J 92(1):87–91

28. Gan Q, Wang T, Cochrane C, McCarron P (2005) Modulation of surface charge, particle size and morphological properties of chitosan–TPP nanoparticles intended for gene delivery. Colloids Surf B 44(2–3):65–73

29. Zhang H, Oh M, Allen C, Kumacheva E (2004) Monodisperse chitosan nanoparticles for mucosal drug delivery. Biomacromolecules 5(6):2461–2468. doi:10.1021/bm0496211

30. Huang Y, Lapitsky Y (2011) Monovalent salt enhances colloidal stability during the formation of chitosan/tripolyphosphate microgels. Langmuir 27(17):10392–10399. doi:10.1021/la201194a

31. Tsai ML, Bai SW, Chen RH (2008) Cavitation effects versus stretch effects resulted in different size and polydispersity of ionotropic gelation chitosan-sodium tripolyphosphate nanoparticle. Carbohyd Polym 71(3):448–457

32. Al-Manasir N, Zhu KZ, Kjoniksen AL, Knudsen KD, Karlsson G, Nystrom B (2009) Effects of temperature and pH on the contraction and aggregation of microgels in aqueous suspensions. J Phys Chem B 113(32):11115–11123. doi:10.1021/jp901121g

33. Schärtl W (2007) Light scattering from polymer solutions and nanoparticle dispersions. Springer, Berlin

34. Siegert AJF (1943) Radiation laboratory report no. 465. MIT, Cambridge, MA, USA

35. López-León T, Carvalho ELS, Seijo B, Ortega-Vinuesa JL, Bastos-González D (2005) Physicochemical characterization of chitosan nanoparticles: electrokinetic and stability behavior. J Colloid Interface Sci 283(2):344–351

36. Tsaih ML, Chen RH (1997) Effect of molecular weight and urea on the conformation of chitosan molecules in dilute solutions. Int J Biol Macromol 20(3):233–240. doi:10.1016/s0141-8130(97) 01165-3

37. de Campos AM, Diebold Y, Carvalho ELS, Sanchez A, Alonso MJ (2004) Chitosan nanoparticles as new ocular drug delivery systems: in vitro stability, in vivo fate, and cellular toxicity. Pharm Res 21:803–810. doi:10.1023/B:PHAM.0000026432.75781.cb

38. Chen W, Hsu C, Huang J, Tsai M, Chen R (2011) Effect of the ionic strength of the media on the aggregation behaviors of high molecule weight chitosan. J Polym Res:1–11. doi:10.1007/s10965-010-9543-9

39. Tanaka H (1992) Appearance of a moving droplet phase and unusual networklike or spongelike patterns in a phase-separating polymer solution with a double-well-shaped phase diagram. Macromolecules 25:6377–6380

40. Tanaka H (1993) Unusual phase separation in a polymer solution caused by asymmetric molecular dynamics. Phys Rev Lett 71 (19):3158–3161

41. Zhang G, Wu C (2006) Folding and formation of mesoglobules in dilute copolymer solutions. Adv Polym Sci 195:101–1076

42. Piçarra S, Martinho JMG (2001) Viscoelastic effects on dilute polymer solutions phase demixing: fluorescence study of a poly (ε-caprolactone) chain in THF. Macromolecules 34(1):53–58. doi:10.1021/ma001231t